

Plasma Lens and Plasma Wakefield Acceleration Experiments Using Twin Linacs

A. Ogata, H. Nakanishi, K. Nakajima, T. Kawakubo, D. Whittum, M. Arinaga
National Laboratory for High Energy Physics (KEK), Oho, Tsukuba, Japan

Y. Yoshida, T. Ueda, T. Kobayashi

Nuclear Engineering Research Laboratory, Faculty of Engineering, The University of Tokyo, Tokai-mura, Ibaraki-ken, Japan

H. Shibata and S. Tagawa

Research Center for Nuclear Science and Technology, The University of Tokyo, Tokai-mura, Ibaraki-ken, Japan

N. Yugami and Y. Nishida

Department of Electrical and Electronic Engineering, Utsunomiya University, Utsunomiya, Japan

Abstract

A collinear wakefield test facility using two linacs with a common test section is constructed. Beams from one linac excite wakefields in a test medium such as a plasma, while beams from the other linac witness the wakefields. The time interval between the two beams is controllable with an accuracy of ~ 1 psec. Plasma wakefield acceleration and plasma lens experiments were conducted using this facility.

1 INTRODUCTION

Plasma wakefield acceleration and plasma lens experiments were conducted using a collinear wakefield test facility[1]. This facility is unique in that it consists of two identical but independent linacs which are called twin-linacs, while in other wakefield accelerators one linac generates both the driving and witness beams. Beams from one linac excite wakefields in a plasma, while beams from the other linac witness the wakefields. The time interval between the two beams is controllable with an accuracy of ~ 1 psec. The plasma lens experiments were conducted using one of the linacs, while the acceleration experiments were conducted using both of them.

2 EXPERIMENTAL APPARATUS

A schematic diagram of the twin linacs is shown in Fig. 1. The part depicted by thick lines has been newly constructed. Each linac can generate beams in three schemes: an isolated single bunch, a 476 MHz bunch train or a 2856 MHz bunch train. Only single isolated bunches were used in these experiments. Because the two beams have different energies, the beamlines were joined in a configuration inverse to that of an energy analyzer. They consist of achromatic lines as shown in Fig. 1, each of which has two dipole magnets and one quadrupole magnet. The two lines share one dipole magnet BM3, *i.e.*, the two lines merge at BM3. Particles with the design energy are focused

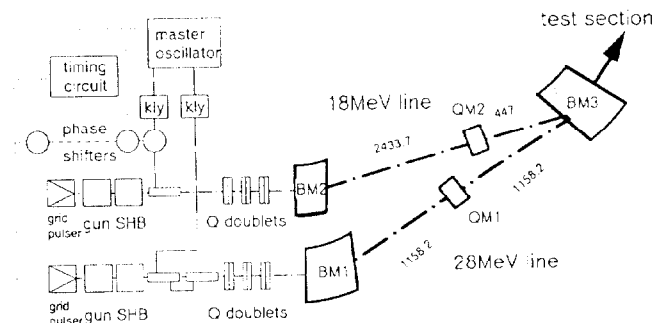


Figure 1: Schematic diagram of the wakefield accelerator. The part depicted by thick lines is newly constructed. Distances between magnets are given in mm. The length of each quadrupole magnet QM_n ($n=1,2$) is 80mm. The distance between two linacs is 750 mm where they are running in parallel.

on the quadrupole magnets (QM1 and QM2 in Fig. 1). The off-energy particles are dispersed by the first dipoles (BM1 and BM2 in Fig. 1), and focused again by QM1 and QM2 onto BM3. Each line has three pairs of doublet quadrupoles upstream, permitting fine tuning of the lattice. The fringe angles of the dipoles are designed so that the β, β' variables at the entrance of the BM1 and BM2 are transposed as $\beta, -\beta'$ at the exit of the BM3. This configuration transports the entire drive beam into the test region without loss due to energy dispersion. It is also possible to introduce witness beams with good energy resolution by inserting a vertical slit at the position of the quadrupole magnet.

To isolate the linacs from the test section, we adopted differential pumping. Previous experience on plasma lens experiments informs us that argon gas is quite harmful to the ion pumps used in the linac main ducts[4]. Nitrogen was adopted as a working gas in these experiments.

Plasmas are produced in a chamber with .3m in diam-

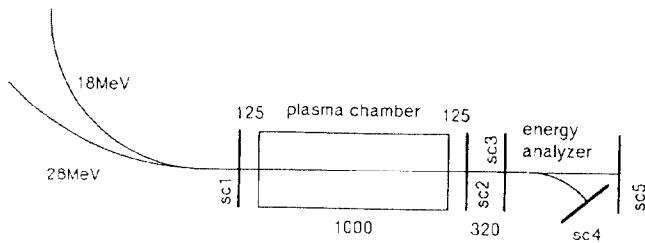


Figure 2: Positioning of phosphor screens.

eter and 1m in length by pulse discharges between four lumps of LaB₆ cathodes and the chamber[2]. The cathodes are heated by a 10V-80A direct current source. The discharge pulse has a voltage of 80-100V, a current of 10-20A, a duration of 2ms and a rate of 6.25Hz equal to the linac beam repetition rate. The multi-dipole field of permanent magnets, 1kG at the inner surface of the water-cooled chamber, is applied to confine the plasma. The base pressure of the chamber is typically 10⁻⁶ torr. The plasma density was controlled both by the gas flow controller and the discharge current. The plasma density and temperature are measured by a Langmuir probe. Though we have no measurement of the density distribution, the measurement on a similar confinement device shows that it is fairly homogeneous both in longitudinal and transverse directions[3].

A 45° bending magnet at the end of the plasma chamber measured the beam energy, giving a displacement of -55.8keVmm⁻¹. Five phosphor screens measured transverse profiles, whose positions are given in Fig. 2.

3 EXPERIMENTAL RESULTS

3.1 Single Beam Experiments

Plasma lens experiments in the overdense regime already have been reported[4]. Here we report those in underdense regime. Experimental conditions were as follows; beam energy was 16MeV, charge of a bunch was 300pC, beam sizes at the first screen (SC1 in Fig. 2) were 1.27mm × 3.13mm × 3mm, electron density n_b at SC1 was 10¹⁰cm⁻³, vertical β, γ functions at SC1 were 0.99m and 1.4m⁻¹, and vertical emittance was 1.64 mm mrad. Transverse beam sizes were measured on SC2 and SC3 as a function of plasma density n_p .

Fig. 3 gives the results of experiments and calculations; the solution of

$$\beta''/2 + K\beta - (1 + \beta'^2/4)/\beta = 0,$$

where $K = 2\pi r_e n_p / \gamma$. This focusing is stronger than that predicted by simulation.

3.2 Two Beam Experiments

The beam energies of drive beams and test beams were 26.76 MeV and 15.98 MeV, respectively, and the respective

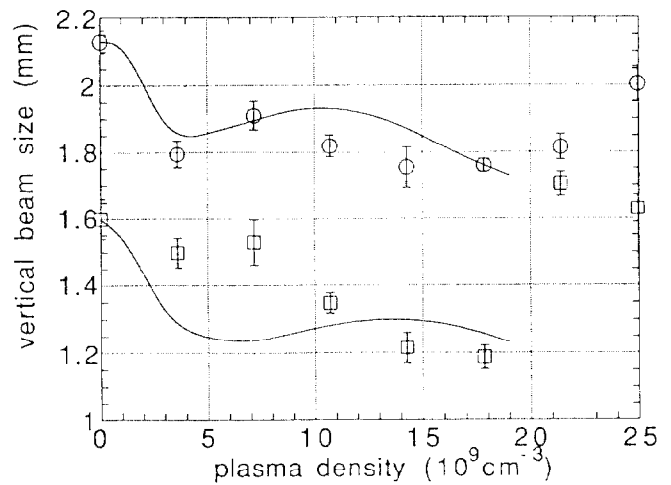


Figure 3: Plasma density dependence of beam sizes on SC2 and SC3. The lines show results of analytical calculation.

charges in each bunch were 300 pC and 15-30 pC. Vertical and horizontal beam sizes of the drive bunch at SC1 are 1.99mm and 0.94mm, respectively, and those of the test bunch were 0.79mm and 0.70mm. Transverse centroids of the two beams coincided at SC1, but they differed 0.5mm vertically and 0.2mm horizontally at SC2.

Beam images on SC5 were observed as a function of time delay between drive and test bunches. A remarkable observation is a periodical, horizontal split of the test bunch, which is shown in Fig. 4. Such an effect would be expected given the incomplete overlap of the two beams. The horizontal distribution is assumed to be sum of two Gaussian distributions. Delay dependence of the centroids of the two components obtained by the least square fit is given in Fig. 5. As for the vertical distribution, the mean and the standard deviation are calculated, which are given in Fig. 6 as position and spread.

The delay dependences were fit to the equation

$$f(t) = e^{-t/\tau} [a_1 \sin(\omega t + \phi_1) + a_2 \sin(2\omega t + \phi_2)].$$

The $\sin 2\omega t$ term is phenomenological, included to improve the fit. The following is a discussion of the parameters in this equation.

1) ω gives the plasma frequency. The plasma density derived from the ω value of the delay dependence of the vertical position is 1.46×10^{11} cm⁻³. This is quite consistent with the value given by the Langmuir probe, 1.5×10^{11} cm⁻³.

2) τ gives the damping time of the oscillation. The same curve gives 3.69nsec. This is very fast.

3) The vertical position is varied only by the transverse wakefield, while the horizontal positions are varied both by the transverse and longitudinal wakefields. Panofski-Wentzel theorem tells there should be $\pi/2$ difference between these two wakefields. Let us consider only the $\sin(\omega t + \phi_1)$ term. The vertical position of Fig. 6 is approximated as $\sin(21.96t - 0.249)$, where t is in nsec. The

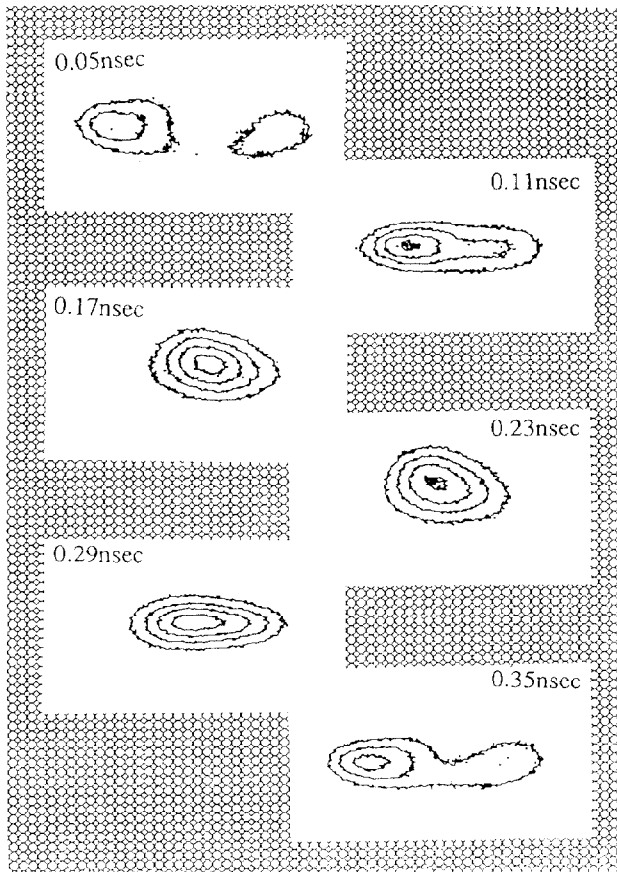


Figure 4: Typical images on SC5.

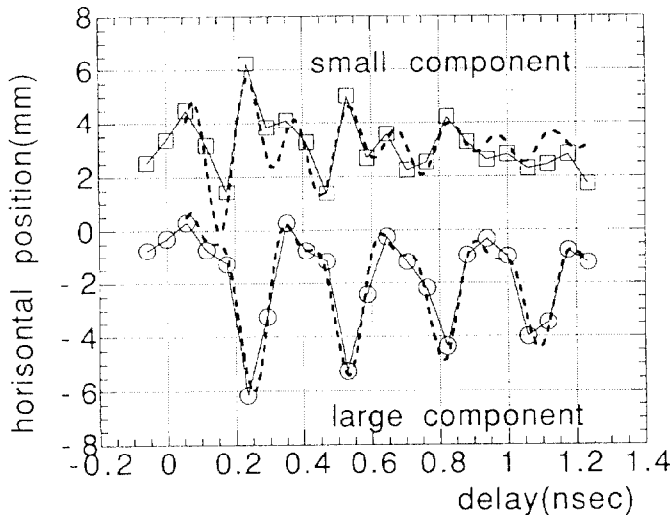


Figure 5: Delay dependence of the horizontal centroid shift of two components.

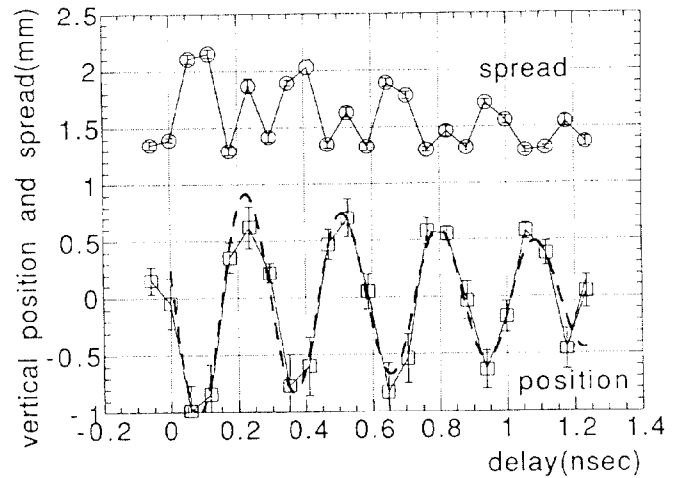


Figure 6: Delay dependence of the vertical position and spread.

small component of Fig. 5 is approximated as $\sin(21.15t - 1.22) = \sin(21.96t - 0.249 - 0.97)$ while the large component is $\sin(22.47t - 0.85) = \sin(21.96t - 0.249 - 0.60)$. The coefficients of t are regarded as the same values. Using the equality $a_t \sin(\omega t + \phi_1) + a_l \cos(\omega t + \phi_1) = (a_t^2 + a_l^2)^{1/2} \sin(\omega t + \phi_1 + \psi)$, $\tan \psi = a_l/a_t$, we can derive the ratio between longitudinal and transverse wakes a_l/a_t from the ψ values. The small component gives $a_l/a_t = \tan(-0.97) = -1.45$ while the large component gives -0.684 .

4) We can derive amplitudes of longitudinal wakefields from a_l and a_t values, which are around 100keV, consistent with the predictions of linear theory.

4 CONCLUSION

Plasma lens and plasma wakefield acceleration experiments were conducted on colinear wakefield test facility. Plasma focusing in the underdense regime was demonstrated. In the acceleration experiments, beam images were observed as a function of time delay between drive and test bunches at the end of an energy analyzer. A periodic, horizontal split of the test bunch is observed. The plasma oscillation decayed with a very short time constant; a few ns. A $2\omega_p$ component also appeared in the oscillation.

5 REFERENCES

- [1] H. Nakanishi *et al.*, Nucl. Instr. Meth., in press.
- [2] K. Nakajima *et al.*, Nucl. Instr. Meth. A292(1990)12.
- [3] Y. Nishida *et al.*, IEEE Trans. Plasma Sci. PS-15(1987)243.
- [4] H. Nakanishi *et al.*, Phys. Rev. Lett. 66(1991)1870; Y. Yoshida *et al.*, Part. Accel. 39(1992)77.